ChemComm

RSC Publishing

COMMUNICATION

View Article Online
View Journal | View Issue

Photoresponsive quinoline tethered fluorescent carbon dots for regulated anticancer drug delivery†

Cite this: *Chem. Commun.*, 2013, **49**, 10471

Received 8th August 2013,
Accepted 15th September 2013

DOI: 10.1039/c3cc46078a

www.rsc.org/chemcomm

S. Karthik,[a] Biswajit Saha,[b] Sudip Kumar Ghosh*[b] and N. D. Pradeep Singh*[a]

A photoresponsive nano drug delivery system (DDS) was constructed using two new ingredients: fluorescent carbon dots and a quinoline based phototrigger. The strong fluorescent properties of carbon dots have been explored for *in vitro* cellular imaging application, and the phototrigger ability of quinoline was exploited for efficient anticancer drug release using both one-photon and two-photon excitation.

Nano drug delivery systems (DDSs) combining both diagnostic and therapeutic capabilities have become an emerging field in the area of nanomedicine.[1] In the past few years, photoresponsive nano DDSs have captured great attention because of their key ability to regulate drug release spatially and temporally by external regulated light.[2] The central challenge involved in the construction of photoresponsive nano DDSs is to design nanoparticles that exhibit both fluorescence and phototrigger properties. In general, nanoparticles utilized for photoresponsive DDSs are constructed using two main ingredients, namely, biocompatible nanoparticles and a small organic chromophore "phototrigger".[3–6] To date, many kinds of nanomaterials, such as gold nanoparticles, iron oxide nanoparticles, silica nanoparticles, and carbon nanotubes, have been well explored as biocompatible nanoparticles for photoresponsive nano DDSs.[7–12] The aforementioned nanoparticles were found to be non-fluorescent in nature. Hence for both fluorescence and photocontrolled release functionalities, we have to depend mainly on the phototrigger component. This consequently reduces our choice to select only phototriggers which can exhibit strong fluorescence, mainly coumarin derivatives. By any means, if we can develop biocompatible fluorescent nanoparticles, then our choice towards phototriggers can be widely expanded.

Recently, fluorescent carbon nanoparticles (FCNs) have become promising candidates in the area of cell imaging and sensing owing to their remarkable properties like stable photoluminescence, tunable excitation and emission wavelength, chemical inertness, water solubility, biocompatibility, and excellent cell membrane permeability due to their small size and tunable surface functionalities.[13,14] Wu and co-workers[15] demonstrated naphthalimide-azide conjugated carbon dots as a fluorescent sensor for the detection of hydrogen sulfide in aqueous media and inside living cells based on FRET chemistry. Furthermore, the same group also developed a fluorescent ratiometric nanosensor for detecting NO in aqueous media using phenylenediamine-containing naphthalimide conjugated carbon dots.[15] Recently, the Chen group constructed photosensitiser (chlorine-e6) tethered carbon dots for simultaneous enhanced fluorescence imaging and photodynamic therapy.[16] Inspired by the unique features of carbon dots such as strong fluorescence, biocompatibility and ease of attachment of organic molecules we were prompted to use carbon dots for the first time as biocompatible fluorescent nanocarriers in the construction of a photoresponsive nano DDS. Herein, we designed fluorescent carbon dots decorated by a phototrigger for simultaneous fluorescent imaging and regulated delivery of anticancer drugs. For the current study, we selected a 7-methoxy quinoline moiety as a phototrigger because of its weak fluorescence and release ability upon both one-photon excitation (1PE) and 2PE.[17]

We synthesized a phototrigger conjugated anticancer drug, 7-(3-bromopropoxy)-2-quinolylmethyl chlorambucil (Qucbl), as shown in Scheme S1 (ESI†). Nitrogen containing carbon dots were prepared by heating citric acid and urea in distilled water in a domestic 750 W microwave oven for 4–5 min, as reported in the literature.[14] Finally, Qucbl was covalently anchored onto the surface of Cdots using potassium *tert*-butoxide in dry THF (Scheme 1). The attachment of Qucbl onto the surface of Cdots was validated by UV-Vis, FT-IR, and ^{13}C NMR spectroscopy and HPLC (Fig. S1–S7, ESI†).

The physicochemical properties of Qucbl-Cdots such as morphology, size, and zeta potential were studied since they have an influence on the cellular uptake. The size and shape of carbon dots were observed by the TEM study. The representative TEM images of Cdots and Qucbl-Cdots are presented in Fig. 1a and b.

Fig. 1a shows that the Cdots were aggregated and globular in nature with an average particle size of ~5–7 nm, and Fig. 1b shows that the Qucbl-Cdots were polymeric in nature with an average particle size of ~60–80 nm. DLS studies revealed that the mean particle sizes of Cdots and Qucbl-Cdots were 4.7 ± 1.6 nm and

[a] *Department of Chemistry, Indian Institute of Technology Kharagpur, Kharagpur–721302, India. E-mail: ndpradeep@chem.iitkgp.ernet.in*
[b] *Department of Biotechnology, Indian Institute of Technology Kharagpur, Kharagpur–721302, India*

† Electronic supplementary information (ESI) available: Details of synthesis and characterization, and other experimental details. See DOI: 10.1039/c3cc46078a

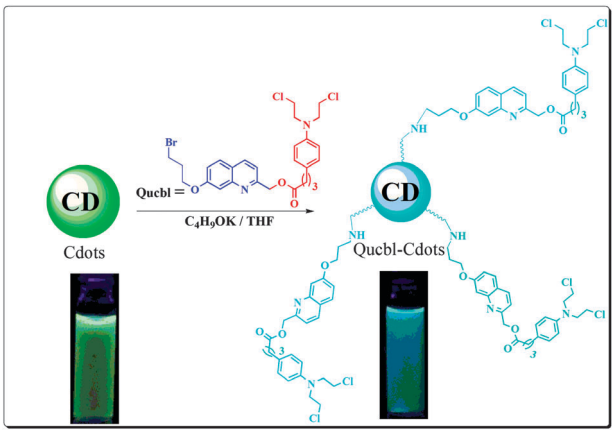

Scheme 1 Synthesis of quinoline-chlorambucil loaded carbon dots (Qucbl-CDs).

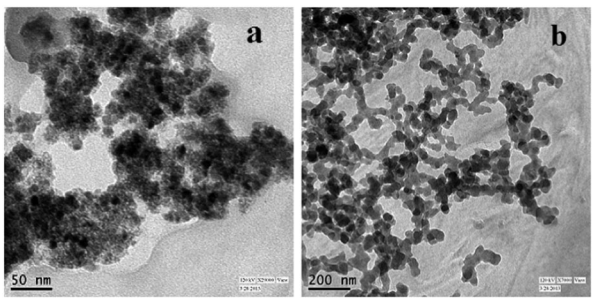

Fig. 1 TEM image of (a) carbon dots and (b) quinoline chlorambucil loaded carbon dots (Qucbl-Cdots).

76.5 ± 1.0 nm (Fig. S9, ESI†), respectively. The increase in particle size of Qucbl-Cdots compared to free Cdots implies that carbon dots were decorated by Qucbl conjugates. This size of the Qucbl-Cdots is well within the preferred range of the nanoparticles used for drug-delivery.[18] The surface functional groups of the C-dots were investigated by FTIR spectroscopy (Fig. S5, ESI†). Broad absorption bands at 3100–3500 cm^{-1} were assigned to (O–H) and (N–H) in Cdots. On the other hand, Qucbl-Cdots showed a decrease in band intensity at 3100–3500 cm^{-1} and a new peak appeared at 2500–2800 cm^{-1} (aromatic C–H stretching), indirectly indicating that QuCbl is loaded on the surface of Cdots. Furthermore, this was also supported by TGA and zeta potentials of the Cdots and the Qucbl-Cdots, which were determined to be +65.3 mV and +31.1 mV, respectively (Fig. S11 and S12, ESI†). The amount of the quinoline chlorambucil loaded on Cdots is calculated to be about ~36 μg mg^{-1}, based on UV-Vis absorption spectra (Fig. S13, ESI†). Qucbl-Cdots showed a broad absorbance from 350 to 450 nm (Fig. 2a) and have a tunable emission from 325 to 550 nm. The emission spectrum of Qucbl-Cdots starts from the visible wavelength range and extends into the near-infrared region (Fig. 2b). It should be noted that a quinoline moiety does not exhibit such tunable emission (Fig. S2, ESI†). Hence, the observed tunable emission of Qucbl-Cdots must be due to the carbon dots. Furthermore, the fluorescent quantum yields of carbon dots and Qucbl-Cdots were found to be 14.0% and 9.9%, respectively (quinine sulphate quantum yield: 54%). Hence, Qucbl-Cdots can be explored for simultaneous cell imaging and photorelease of the anticancer drug. To check the stability of the Qucbl-Cdots in the culture medium, we dispersed the drug loaded Cdots with 10% fetal

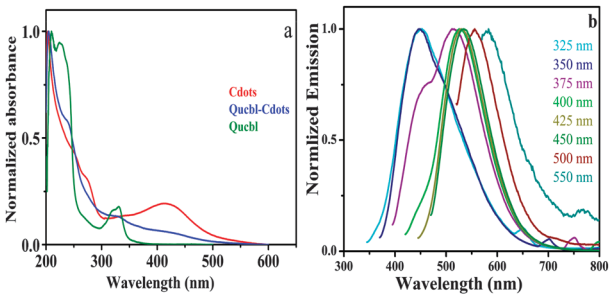

Fig. 2 (a) Normalized absorption spectra of carbon dots (Cdots), quinoline chlorambucil (Qucbl) and quinoline chlorambucil loaded carbon dots (Qucbl-Cdots). (b) Normalised tunable emission spectra of quinoline chlorambucil loaded carbon dots in water.

bovine serum and incubated them at 37 °C in the dark for 96 h. We observed insignificant (2–3%) release of the drug, which proves that the Qucbl-Cdots are quite stable in the dark (Table S2, ESI†).

The time courses of the anticancer drug release by Qucbl-Cdots under photolysis using both UV light (≥365 nm, Hg-vapor lamp) and two-photon 632 nm red light were monitored by reverse phase HPLC. The HPLC profile indicates that ≈73% and 20% of drug release was achieved using both UV and red laser light. After 30 min of irradiation, 73% of the loaded anticancer drug chlorambucil (Fig. S14, ESI†) was effectively released by using UV light ($\lambda \geq 365$ nm, 120 mW cm^{-2}), whereas 20% of the drug was released using a He–Ne laser (5 mW cm^{-2}), suggesting that the external light intensity could regulate the drug release. Furthermore, we also demonstrated precise control of the photolytic release of the loaded anticancer drug by monitoring the release of chlorambucil after periods of exposure to light and dark conditions, as shown in the inset of Fig. S14 (ESI†). The inset clearly shows that the drug release proceeded only under illumination. Furthermore, the photochemical quantum yields of Qucbl and Qucbl-Cdots were calculated to be 0.29 and 0.17, respectively.

Cellular localization of Qucbl-Cdots: to establish that Qucbl-Cdots can be used as a versatile photoresponsive nano DDS, we studied the cellular uptake of drug-loaded Qucbl-Cdots by cancerous HeLa cells. Cells were incubated with 4×10^{-5} M of Qucbl-Cdots in cell culture medium for 4 h and monitored by using fluorescence microscopy. After 4 h of incubation with Qucbl-Cdots, cells showed bright green fluorescence and aggregation of nanoparticles in the cytoplasm and nucleus (Fig. 3a and b). To further confirm the localization of the Qucbl-Cdots inside the nucleus, we stained the cell nuclei with DAPI. We found that the nanoparticles were preferentially located at the nucleus (Fig. 3c and d) as detected by confocal microscopy.

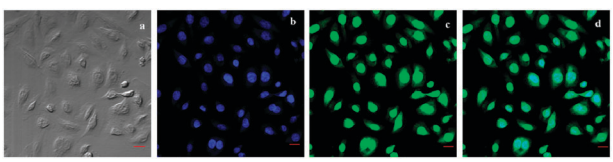

Fig. 3 Confocal images of HeLa cells: (a) brightfield image, (b and c) cells were incubated with 20 μM Qucbl-Cdots for 4 h and cell nuclei were stained using DAPI, (b) showing the uptake of DAPI (25 nM, λ_{ex} = 488 nm), (c) showing the uptake of Qucbl-Cdots (λ_{ex} = 488 nm), (d) overlay image of (b) and (c) showing that both Qucbl-Cdots and DAPI are located at the cell nuclei, the green emission is from Qucbl-Cdots and the blue emission is from DAPI (scale bar = 20 μm).

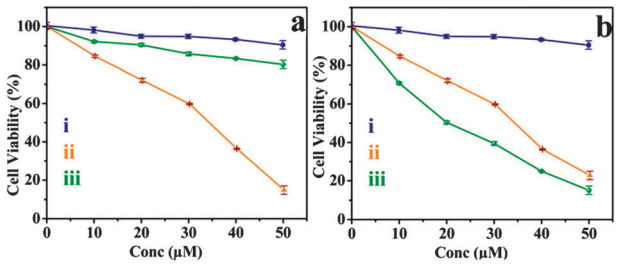

Fig. 4 (a and b) Cell viability test of (i) Cdots, (ii) chlorambucil (iii) Qucbl-Cdots in the HeLa cell line: (a) before irradiation (b) after irradiation and values are presented as mean ± SD.

Furthermore, to explore the tunable emission properties of Qucbl-Cdots, we carried out cellular imaging at two different excitation wavelengths (488 nm and 569 nm), and the results are presented in Fig. S15 (ESI†). After successful demonstration of pronounced accumulation of Qucbl-Cdots within the nucleus of HeLa cells, we evaluated the cytotoxicity of Qucbl-Cdots, chlorambucil and Cdots *in vitro* using the MTT assay in the HeLa cell line. Cytotoxicity was expressed as the percentage of cell viability relative to the untreated control cells. The percentage of cell viability was plotted *versus* the concentration. It was observed that cell viability remains above 90% at different concentrations of Qucbl-Cdots and Cdots, whereas an increase in cytotoxicity was observed upon addition of increasing amounts of chlorambucil (Fig. 4a). In the light exposure experiment, incubation of cells with different concentrations of Qucbl-Cdots upon irradiation for 30 min under UV light (≥365 nm) resulted in the release of the anticancer drug chlorambucil, thereby causing cytotoxicity in cancerous HeLa cells as validated by the MTT toxicity data (Fig. 4b), and the cell death of HeLa cells was further confirmed by cell cycle analysis. On the other hand, there was no significant cell death observed when the cells were irradiated in the presence of Cdots, indicating that the cytotoxicity was likely caused by the released drug, chlorambucil, upon light irradiation. On comparison with the same concentration of chlorambucil as that of Qucbl-Cdots, Qucbl-Cdots showed much lower cytotoxicity compared to chlorambucil. But upon irradiation, Qucbl-Cdots showed an enhanced cytotoxicity to cancer cells in comparison to chlorambucil, because of the efficient photorelease of chlorambucil inside the cell. Furthermore, to validate the ability of photocaged Qucbl-Cdots to be used for externally regulated drug release, the HeLa cells incubated with 2×10^{-5} M Qucbl-Cdots were exposed to UV light (≥365 nm) for different time intervals. We found that the cytotoxicity toward HeLa cells at an irradiation time of 30 min resulted in the highest level of toxicity, indicating that most of the drugs were released from the Cdots (Fig. S16, ESI†).

Chlorambucil induced cell death in HeLa cells was also demonstrated by cell cycle analysis. The percentage of controlled cell death was calculated using a FACS calibur flow cytometer. As shown in Fig. S17 (ESI†), 6.93 ± 0.56% of cell death was found in untreated control cells, whereas cells treated with chlorambucil, Qucbl-Cdots, and Cdots showed 22.76 ± 0.17%, 28.21 ± 0.24% and 9.37 ± 0.83% of cell death, respectively, at 48 h, after exposure to UV light for 30 min. It is evident that free chlorambucil and Qucbl-Cdots induced more cell death than Cdots. The higher cell death activity of Qucbl-Cdots than free chlorambucil suggests that chlorambucil-loaded carbon dots can efficiently enhance the intracellular drug delivery for a sustained period of time.

In summary, we have developed fluorescent carbon dots tethered to a quinoline based phototrigger for regulated delivery of anticancer drugs. The fluorescence properties of Cdots have been explored for *in vitro* cellular imaging application. The photoregulated drug release ability of Qucbl-Cdots has been established by means of periodic exposure to light and dark conditions. Furthermore, Qucbl-Cdots were readily internalized inside the HeLa cells and showed precise control over the drug release to kill the cancer cells upon irradiation. Although our photoresponsive Qucbl-Cdots are effective for regulated drug delivery, their application for *in vivo* studies is still restricted due to their absorbance below 500 nm. Hence, in future we wish to design photoresponsive Cdots which can be operated in the NIR region.

We thank Dr Roy Chaudhuri for providing the He–Ne laser for photolysis. DST-SERB for financial support. DST-FIST for 400 MHz NMR. S. Karthik is thankful to IIT KGP for the fellowship.

Notes and references

1 N. Nasongkla, E. Bey, J. Ren, H. Ai, C. Khemtong, J. S. Guthi, S. F. Chin, A. D. Sherry, D. A. Boothman and J. Gao, *Nano Lett.*, 2006, **6**(11), 2427.
2 M. S. Yavuz, Y. Cheng, J. Chen, C. M. Cobley, Q. Zhang, M. Rycenga, J. Xie, C. Kim, K. H. Song, A. G. Schwartz, L. V. Wang and Y. Xia, *Nat. Mater.*, 2009, **8**, 935.
3 S. S. Agasti, A. Chompoosor, C. You, P. Ghosh, C. K. Kim and V. M. Rotello, *J. Am. Chem. Soc.*, 2009, **131**, 5728; Y. Zhu and M. Fujiwara, *Angew. Chem., Int. Ed.*, 2007, **46**, 2241.
4 N. K. Mal, M. Fujiwara and Y. Tanaka, *Nature*, 2003, **421**, 350; J. Babin, M. Pelletier, M. Lepage, J. Allard, D. Morris and Y. Zhao, *Angew. Chem., Int. Ed.*, 2009, **48**, 3329.
5 Q. Lin, Q. Huang, C. Li, C. Bao, Z. Liu, F. Li and Z. Linyong, *J. Am. Chem. Soc.*, 2010, **132**, 10645; N. Knezevic, B. G. Trewyn and V. S.-Y. Lin, *Chem. Commun.*, 2011, **47**, 2817.
6 N. Knezevic, B. G. Trewyn and V. S.-Y. Lin, *Chem.–Eur. J.*, 2011, **17**, 3338; G. Liu and C.-M. Dong, *Biomacromolecules*, 2012, **13**, 1573.
7 V. P. Torchilin, *Pharm. Res.*, 2007, **24**, 1; R. Savic, L. Luo, A. Eisenberg and D. M. Maysinger, *Science*, 2003, **300**, 615; H. Koo, H. Lee, S. Lee, K. H. Min, M. S. Kim, D. S. Lee, Y. Choi, I. C. Kwon, K. Kim and S. Y. Jeong, *Chem. Commun.*, 2010, **46**, 5668.
8 J. Kim, Y. Piao and T. Hyeon, *Chem. Soc. Rev.*, 2009, **38**, 372; Y. W. Jun, J. H. Lee and J. Cheon, *Angew. Chem., Int. Ed.*, 2008, **47**, 5122.
9 S. Lee, E.-J. Cha, K. Park, S. Y. Lee, J. K. Hong, I. C. Sun, S. Y. Kim, K. Choi, I. C. Kwon, K. Kim and C. H. Ahn, *Angew. Chem., Int. Ed.*, 2008, **47**, 2804; X. M. Qian and S. M. Nie, *Chem. Soc. Rev.*, 2008, **37**, 912.
10 S. R. Ji, C. Liu, B. Zhang, F. Yang, J. Xu, J. Long, C. Jin, D. l. Fu, Q. x. Ni and X. j. Yu, *Biochim. Biophys. Acta, Rev. Cancer*, 2010, **1806**, 29; N. W. S. Kam, M. O'Connell, J. A. Wisdom and H. Dai, *Proc. Natl. Acad. Sci. U. S. A.*, 2005, **102**, 11600.
11 K. Tanaka, N. Kitamura and Y. Chujo, *Bioconjugate Chem.*, 2011, **22**, 1484; M. Benezra, O. Penate-Medina, P. B. Zanzonico, D. Schaer, H. Ow, A. Burns, E. DeStanchina, V. Longo, E. Herz, S. Iyer, J. Wolchok, S. M. Larson, U. Wiesner and M. S. Bradbury, *J. Clin. Invest.*, 2011, **121**, 2768.
12 D.-E. Lee, H. Koo, I.-C. Sun, J. H. Ryu, K. Kim and I.-C. Kwon, *Chem. Soc. Rev.*, 2012, **41**, 2656; S. Karthik, N. Puvvada, B. N. P. Kumar, S. Rajput, A. Pathak, M. Mandal and N. D. P. Singh, *ACS Appl. Mater. Interfaces*, 2013, **5**, 5232.
13 S. k. Md Palashuddin, A. Jaiswal, A. Paul, S. S. Ghosh and A. Chattopadhyay, *Sci. Rep.*, 2012, **2**, 383; S. K. Bhunia, A. Saha, A. R. Maity, S. C. Ray and N. R. Jana, *Sci. Rep.*, 2013, **3**, 1473.
14 S. N. Baker and G. A. Baker, *Angew. Chem., Int. Ed.*, 2010, **49**, 6726; S. Qu, X. Wang, Q. Lu, X. Liu and L. Wang, *Angew. Chem., Int. Ed.*, 2012, **51**, 1.
15 C. Yu, X. Li, F. Zheng and S. Wu, *Chem. Commun.*, 2013, **49**, 403; C. Yu, Y. Wu, F. Zeng and S. Wu, *J. Mater. Chem. B.*, 2013, **1**, 4152.
16 P. Huang, J. Lin, X. Wang, Z. Wang, C. Zhang, M. He, K. Wang, F. Chen, Z. Li, G. Shen, D. Cui and X. Chen, *Adv. Mater.*, 2012, **24**, 5104.
17 Y. Zhu, C. M. Pavlos, P. Toscano and T.M. Dore, *J. Am. Chem. Soc.*, 2006, **128**, 4267; L. Yi-Ming, J. Shi, R. Cai, X.-Y. Chen, Q.-X. Guo and L. Liu, *Tetrahedron Lett.*, 2010, **5**, 11609.
18 A. H. Faraji and P. Wipf, *Bioorg. Med. Chem.*, 2009, **17**, 2950.